Research Article

Muhammad Javaid and Aqsa Sattar*

On topological indices of zinc-based metal organic frameworks

https://doi.org/10.1515/mgmc-2022-0010
received February 09, 2022; accepted May 09, 2022

Abstract: Metal organic frameworks (MOFs) are distinctive porous chemical materials comprised of metal ions and organic ligands to illustrate marvelous chemical stability, high surface area, distinctive morphology, and large pore volume. MOFs have great significance due to their versatile utilizations, such as purification and separation of various gases, environmental hazards, biocompatibility, toxicology, heterogeneous catalyst, and biomedical applications. These structures have attracted global attention of researchers due to their increasing utilizations in many areas of science. Freshly, zinc-based MOFs are becoming popular because of their versatile application in biomedical, i.e., drug delivery, biosensing, and cancer imaging. Topological indices (TIs), the graphs invariants or numerical graph descriptors, are useful in characterizing the topology of molecular structures and helpful in defining the psychochemical properties of these structures. This paper mainly highlights the comparison between two MOFs namely zinc oxide (ZnOx) and zinc silicate (ZnSl) networks via some multiplicative Zagreb connection indices (MZIs), namely modified first MZCI (1st MZCI) modified second MZCI (2nd MZCI), and modified third MZCI (3rd MZCI).

Keywords: metal organic frameworks, connection numbers, multiplicative Zagreb indices

1 Introduction

Metal organic frameworks (MOFs) are uniformly organized distinctive porous chemical coordinated compounds made up of metal clusters and organic linkers. MOFs have wide-ranging utilizations such as purification and separation of various gases, environmental hazards, biocompatibility, toxicology, heterogeneous catalyst, and biomedical applications. Their precise structure, extensive range of pore formation, large surface area, high porosity, tunable frameworks, relatively low toxicity, and simple chemical functionalization have made them a promising applicant for drug delivery, nitric oxide storage, imaging and sensing, and disease diagnosis. Biomedical applications have recently emerged as an intriguing and promising area for the development and implementation of multi-functional MOFs. Drug delivery in an efficient way is one of the important points in this field. Non-toxic MOFs are considered to be more efficient rather than toxic MOFs in biological applications, especially in drug delivery systems. The antibacterial activity of MOFs based on non-toxic antimicrobial cations (Zn^{2+}) was newly discussed (Taghipour et al., 2018, Wang et al., 2011). Zinc-based MOFs are investigated into biomedical applications due to the low toxicity of zinc ions. Zinc ion is broadly utilized in dermatology, moisturizing the skin and as cicatrizing agent (Prasad, 2008). In addition, biomedical utilizations with their biocompatibility, and toxicology described the production methods of zinc-based MOFs. Kashif et al. (2021) discussed M-polynomial TIs of MOFs. Recently, Ahmad et al. (2022) found the polynomial of degree-based indices of MOFS. For more study, the readers are referred to the study by Abbas et al. (2021), Awais et al. (2020), and Chu et al. (2020).

MOFs have ability to predict many chemical and physical properties other than detecting and sensing, such as biosensor increasing response time, selectivity, and sensitivity (Ding et al., 2017), impregnating appropriate active materials (Thornton et al., 2009), changing photosynthetic and organic legends (Yin et al., 2015), grafting (Hwang et al., 2008), and ion exchange (Kim et al., 2012). MOFs have a vast range of utilizations such as to separate and purify the chemical compounds (Lin et al., 2019) and to store energy in batteries (Xu et al., 2017). Yap et al. (2017) recently utilized MOFs as precursors to prepare distinct nanostructures. Graph theory is playing vital role in

* **Corresponding author: Aqsa Sattar,** Department of Mathematics, School of Science, University of Management and Technology (UMT), Lahore 54770, Pakistan, e-mail: sattaraqsa47@gmail.com
Muhammad Javaid: Department of Mathematics, School of Science, University of Management and Technology (UMT), Lahore 54770, Pakistan, e-mail: javaidmath@gmail.com

Open Access. © 2022 Muhammad Javaid and Aqsa Sattar, published by De Gruyter. This work is licensed under the Creative Commons Attribution 4.0 International License.

providing the tools to predict the distinct physicochemical properties such as flash point, temperature, boiling and freezing point, density, and pressure of various chemical structures in modern chemistry. Wiener (1947) discovered the first distance-based TI to study the boiling point of paraffin. Further, Gutman and Trinajstic (1972) put forward the first degree-based TI to check the total π-electron energy of alternant hydrocarbon. The conception of second degree-based TI was investigated by Gutman et al. (1975). Further, the concept of third ZI was initiated by Furtula and Gutman (2015). Later, Nikolic et al. (2003) introduced the notion of modified first ZI in 2003. Dhanalakshmi et al. (2016) put forward the idea of multiplicative ZI (MZI). Dustigeer et al. (2020) calculated the computed degree-based MZIs of planer octahedron networks. These classical ZI have been employed widely in the domain of cheminformatics (Ali et al., 2018; Javaid and Imran, 2021; Rao et al., 2021).

Later on, Ali and Trinajstić (2018) introduced a new term called connection number (number of vertices at distance two) and investigated connection-based ZI (ZCIs). Freshly, Ali et al. (2020) calculated the modified ZCIs for T-sum graphs in 2020. Haoer et al. (2020) introduced the concept of multiplicative leap ZIs. Javaid et al. (2021) introduced the idea of multiplicative ZCIs (MZCI) and computed the general expressions to find these connection-based indices of different wheel-related graphs. Li et al. (2021) computed modified ZIs of some chemical structures. Further, Gao et al. (2020) calculated ZIs of dendrimers in 2020. Recently, Sattar et al. (2021, 2022) developed the general expressions to compute the MZCIs of dendrimer nanostars. Further, Zhao et al. (2021) calculated the topological co-indices of MOFs.

For more understanding, the readers are referred to the study by Siddiqui et al. (2021) and Zahra and Ibrahim (2021). The motivation to this research article is as follows:

1. MOFs, the uniformly organized distinctive porous chemical coordinated compounds, have great significance due to their vast range of utilizations. Zinc-based MOFs have been widely utilized in biomedical applications such as drug delivery, biosensing, and cancer imaging.
2. TIs, the numerical graph descriptors are useful in characterizing the topology of molecular structures and helpful in defining the psychochemical properties of these structures.
3. The ZCI, rather than the other classical degree and distance-based ZIs, have better applicability to specify the physical and chemical properties of molecular structures.

In this paper, we work to calculate the MZCIs of two distinct zinc-based MOFs, namely zinc oxide (ZnOx) and zinc silicate (ZnSl) graphs. We also compare the results of both ZnOx and ZnSl networks to check the superiority of proposed expressions.

This manuscript is structured as; in Section 2, we state the related definitions from the literature which assist the reader to understand the idea of this manuscript. Section 3 involves the main result to compute the multiplicative ZCIs for zinc oxide-related MOFs. In Section 4, we compute the main results for zinc silicate-related MOFs in a very comprehensive way. Section 5 involves the comparative study between ZnOx- and ZnSl-related MOFs and the concluding remarks of this article.

2 Preliminaries

This section involves some useful basic definitions from the literature to understand the main results of this manuscript.

Definition 2.1. Let $Q = (X(Q), T(Q))$ be a graph, where $X(Q)$ and $T(Q)$ be the vertex set and edge set, respectively (Gutman and Trinajstic, 1972). Then, the ZIs on the bases of degree are defined as:

1. $Z_1(Q) = \sum_{m\in X(Q)}(\boldsymbol{d_Y}(m))^2 = \sum_{mz\in T(Q)}(\mathbf{d}_Q(m) + \mathbf{d}_Q(z))$,
2. $Z_2(Q) = \sum_{mz\in T(Y)}(\boldsymbol{d}_Q(m) \times \boldsymbol{d}_Q(z))$,

where $\boldsymbol{d}_Q(m)$ and $\boldsymbol{d}_Q(z)$ are the degrees of the vertex m and z, respectively. These ZIs are called first ZI and second ZI, respectively.

Definition 2.2. For a graph Q, the connection-based ZIs can be defined as (Ali and Trinajstić, 2018):

1. $\mathrm{ZC}_1(Q) = \sum_{m\in X(Q)}(\omega_Q(m))^2$,
2. $\mathrm{ZC}_2(Q) = \sum_{mz\in T(Q)}(\omega_Q(m) \times \omega_Q(z))$,

where $\omega_Q(m)$ and $\omega_Q(z)$ is the connection number (CN) of the vertex m and z, respectively. These ZCIs are called first Zagreb connection index (1st ZCI) and second Zagreb connection index (2nd ZCI), respectively.

Definition 2.3. For a graph Q, the modified ZCIs can be given as (Ali et al., 2020):

1. $ZC_1^{\star}(Q) = \sum_{m\in T(Q)}(\omega_Q(m) + \omega_Q(z)) = \sum_{m\in X(Q)}(\boldsymbol{d}_Q(m)\omega_Q(m))$,
2. $ZC_2^{\star}(Q) = \sum_{mz\in T(Q)}[d_Q(m)\omega_Q(z) + d_Q(z)\omega_Q(m)]$,
3. $ZC_3^{\star}(Q) = \sum_{mz\in T(Q)}[d_Q(m)\omega_Q(m) + d_Q(z)\omega_Q(z)]$.

These modified ZIs are known as the modified 1st ZCI, modified 2nd ZCI, and modified 3rd ZCI, respectively.

Definition 2.4. For a graph Q, multiplicative ZCIs (MZCI) can be defined as (Kim et al., 2012):

1. $Z^MC_1(Q) = \prod_{m\in X(Q)}(\omega_Q(m))^2$,
2. $Z^MC_2(Q) = \prod_{mz\in T(Q)}(\omega_Q(m) \times \omega_Q(z))$,
3. $Z^MC_3(Q) = \prod_{m\in X(Q)}\boldsymbol{d_Q}(m)\omega_Q(m)$,
4. $Z^MC_4(Q) = \prod_{mz\in T(Q)}(\omega_Q(m) + \omega_Q(z))$.

These MZCIs are known as first MZCI (1st MZCI), second MZCI (2nd MZCI), third MZCI (3rd MZCI), and fourth MZCI (4th MZCI), respectively.

Definition 2.5. For a graph Q, modified first MZCI (1st MZCI), modified second MZCI (2nd MZCI), and modified third MZCI (3rd MZCI) can be given as (Kim et al., 2012):

1. $Z^MC_1^{\star}(Q) = \prod_{mz\in T(Q)}[\boldsymbol{d_Q}(m)\omega_Q(z) + \boldsymbol{d_Q}(z)\omega_Q(m)]$,
2. $Z^MC_2^{\star}(Q) = \prod_{mz\in T(Q)}[\boldsymbol{d_Q}(m)\omega_Q(m) + \boldsymbol{d_Q}(z)\omega_Q(z)]$,
3. $Z^MC_3^{\star}(Q) = \prod_{mz\in T(Q)}[\boldsymbol{d_Q}(m)\omega_Q(m) \times \boldsymbol{d_Q}(z)\omega_Q(z)]$.

Now, we rewrite the modified 1st MZCI, modified 2nd MZCI, and modified 3rd MZCI below.

Definition 2.6. Let Q be a graph and N be a set of all the CNs of the graph Q. Then modified 1st MZCI can be rewritten as:

$$Z^MC_1^{\star}(Q) = \prod_{\substack{\lambda\le\beta\in N\\ \mu\le\nu\in N}}[\mu\beta + \nu\lambda]^{|B_{(\mu,\nu)(\lambda,\beta)}(Q)|} \tag{1}$$

where (α, β) are CNs such that $\alpha \le \beta$ and $\alpha, \beta \in N$ and (μ, ν) are degrees such that $\mu \le \nu$ and $\mu, \nu \in N$. The modified 2nd MZCI can be rewritten as:

$$Z^MC_2^{\star}(Q) = \prod_{\substack{\lambda\le\beta\in N\\ \mu\le\nu\in N}}[\mu\lambda + \nu\beta]^{|B_{(\mu,\nu)(\lambda,\beta)}(Q)|} \tag{2}$$

The modified 3rd MZCI can be rewritten as follows:

$$Z^MC_3^{\star}(Q) = \prod_{\substack{\lambda\le\beta\in N\\ \mu\le\nu\in N}}[\mu\lambda \times \nu\beta]^{|B_{(\mu,\nu)(\lambda,\beta)}(Q)|} \tag{3}$$

where $|B_{(\mu,\ \nu)(\lambda,\ \beta)}(Q)|$ is the total number of edges in Q with degrees (μ, ν) and CNs (λ, β).

3 Connection-based ZIs of zinc oxide

This section includes all the main results for modified 1st MZCI, modified 2nd MZCI, and modified 3rd MZCI of molecular graph of zinc oxide of growth a. Let $\Psi = \mathrm{ZnOx}(a)$ be a molecular graph of zinc oxide of growth a. The cardinality of the vertices and edges of the molecular graph Ψ is $70a + 46$ and $85a + 55$, respectively. The connection-based molecular graph of ZnOx for $a = 1, 2, 3$ is depicted in Figures 1–3.

For our ease, we divide the structure of ZnOx into diamond structure of hexagons, star structure of hexagon, and ξ-hexagons:

1. Diamond structure of hexagons: A structure in which four hexagons are joined in such a way that they have one common vertex having CN 8 and two outer vertices having CN 2 is considered to be diamond structure of hexagons.
2. Star structure of hexagons: A structure in which four hexagons are joined in such a way that they have one common vertex having CN 8 and one outer vertex having CN 2 is considered to be star structure of hexagons.
3. ξ-hexagon: The hexagon which is not part of either diamond or star structure of hexagons is considered to ξ-hexagon of hexagons.

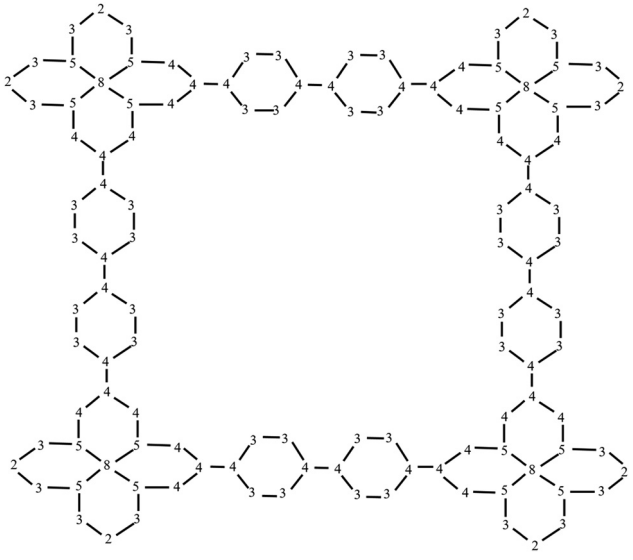

Figure 1: Molecular structure of ZnOx graph for $a = 1$.

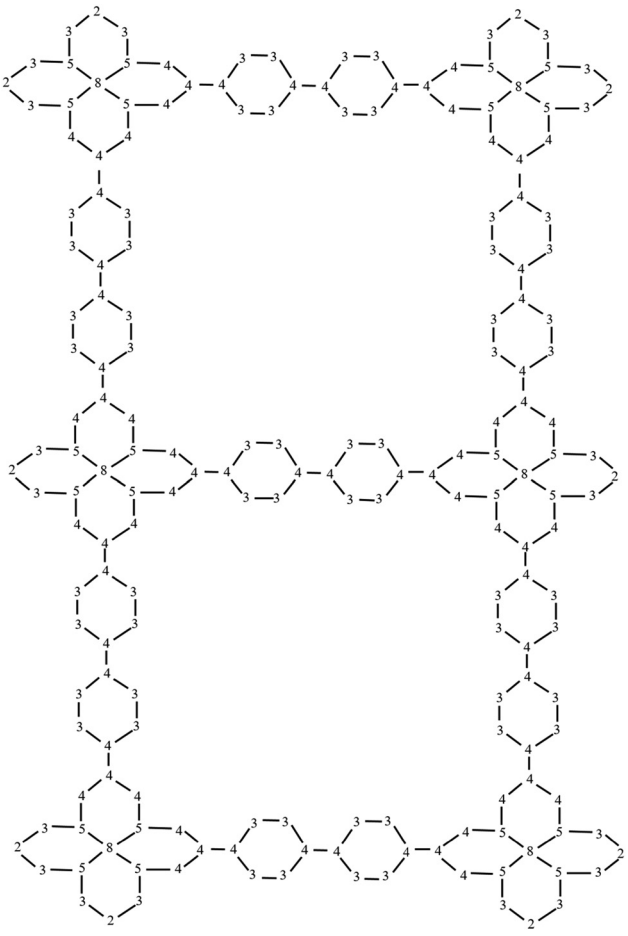

Figure 2: Molecular structure of ZnOx graph for $a = 2$.

The number of diamond structures of hexagons, star structures of hexagons and D structure of hexagons are given in following:

- Number of diamond structure of hexagons = 4,
- Number of star structure of hexagons = $2a - 2$,
- Number of ξ hexagons = $6a + 2$.

Theorem 3.1. *Let $\Psi = ZnOx$ be a molecular structure of zinc oxide graph of growth $a \geq 1$. Then, the expression to compute the modified 1st MZCI is given as*:

$$Z^M C_1^\star(\Psi) = [190]^{4a+12} \times [7128]^{12a+4} \times [20]^{33a+11} \times [44]^{8a+8}$$

Proof. First, we make the partitions of edges with respect to the degrees of incident vertices. There are following four partitions of edges with respect to the degrees of incident vertices:

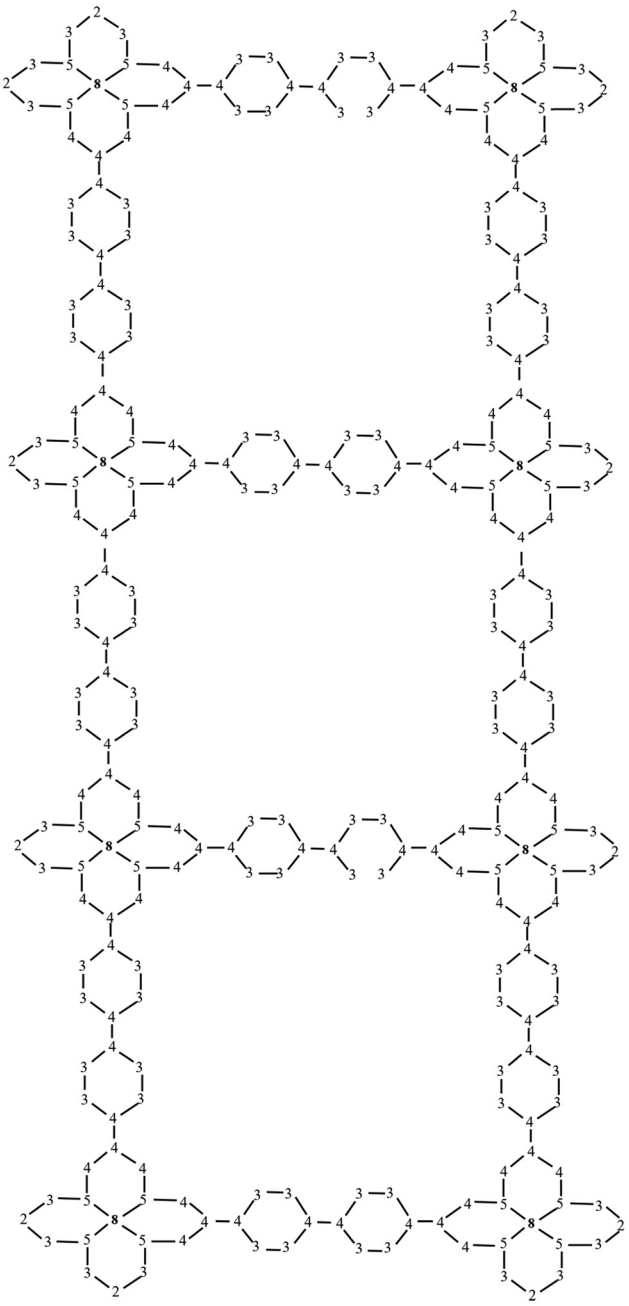

Figure 3: Molecular structure of ZnOx graph for $a = 3$.

$$P_1^e = B_{2,2}^d(\Psi) = \{e = mz \in T : d_\Psi(m) = 2, d_\Psi(z) = 2\}$$
$$P_2^e = B_{2,3}^d(\Psi) = \{e = mz \in T : d_\Psi(m) = 2, d_\Psi(z) = 3\}$$
$$P_3^e = B_{3,3}^d(\Psi) = \{e = mz \in T : d_\Psi(m) = 3, d_\Psi(z) = 3\}$$
$$P_4^e = B_{3,4}^d(\Psi) = \{e = mz \in T : d_\Psi(m) = 3, d_\Psi(z) = 4\}$$

The cardinalities of these partitioned vertices are given below:

$$|B^d_{2,2}(\Psi)| = 6a + 16$$
$$|B^d_{2,3}(\Psi)| = 52a + 28$$
$$|B^d_{3,3}(\Psi)| = 9a + 3$$
$$|B^d_{3,4}(\Psi)| = 8a + 8$$

Now, we divide the edges of Ψ based on their CNs. We have the following seven partitions for the edges as given below:

$P^e_1 = B_{2,3}(\Psi) = \{e = mz \in T : \vartheta_\Psi(m) = 2, \vartheta_\Psi(z) = 3\}$
$P^e_2 = B_{3,3}(\Psi) = \{e = mz \in T : \vartheta_\Psi(m) = 3, \vartheta_\Psi(z) = 3\}$
$P^e_3 = B_{3,4}(\Psi) = \{e = mz \in T : \vartheta_\Psi(m) = 3, \vartheta_\Psi(z) = 4\}$
$P^e_4 = B_{3,5}(\Psi) = \{e = mz \in T : \vartheta_\Psi(m) = 3, \vartheta_\Psi(z) = 5\}$
$P^e_5 = B_{4,4}(\Psi) = \{e = mz \in T : \vartheta_\Psi(m) = 4, \vartheta_\Psi(z) = 4\}$
$P^e_6 = B_{4,5}(\Psi) = \{e = mz \in T : \vartheta_\Psi(m) = 4, \vartheta_\Psi(z) = 5\}$
$P^e_7 = B_{5,8}(\Psi = \{e = mz \in T : \vartheta_\Psi(m) = 5, \vartheta_\Psi(z) = 8\}$

Next, we compute $|B_{2,3}(\Psi)|$. One can easily see that (2,3)-type edges exist in diamond and star structure of hexagons. The number of (2,3)-type edges in diamond structure is four, while in star structure, it is 2.

Thus, we have:

$|B_{(2,3)}(\text{diamond structure of hexagon} = 4 \times 4 = 16$
$|B_{(2,3)}(\text{star structure of hexagons})| = 2(2a - 2)$
$|B_{(2,3)}(\Psi) = 16 + 4a - 4, = 4a + 12$

Next, we compute $|B_{3,3}(\Psi)|$. As it can be seen that only the ξ-hexagons contain the (3,3)-type edges in Ψ. Thus, we have:

$$|B_{(3,3)}(\xi\text{-hexagon})| = 2(6a + 2)$$
$$|B_{(3,3)}(\Psi)| = 12a + 4$$

Similarly, we can calculate the other edges. The cardinalities of the other type of edges are:

$$|B_{3,4}(\Psi)| = 24a + 8, \quad |B_{3,5}(\Psi)| = 4a + 12$$
$$|B_{4,4}(\Psi)| = 4a + 12, \quad |B_{4,5}(\Psi)| = 12a + 4$$
$$|B_{5,8}(\Psi)| = 8a + 8$$

Now, in order to compute modified 1st MZCI, modified 2nd MZCI, and modified 3rd MZCI, we split the partitioned degree-based edges with respect to the connection-based edges.

Table 1 shows the cardinality of edges with degree (μ,ν) and CNs (λ, ϑ). By placing the values of $|B\_(\mu, \nu)(\lambda, \vartheta)(\Psi)|$ in Eq. 1, we have:

$$\begin{aligned}
Z^M C_1^\star(\Psi) = \prod_{\substack{\lambda\le\beta\in N\\ \mu\le\nu\in N}} [\mu\beta + \nu\lambda]^{|B_{(\mu,\nu)(\lambda,\beta)}(\Psi)|} &= [(2)(3) + (2)(2)]^{|B_{(2,2)(2,3)}(\Psi)|} \times [(2)(3) + (2)(3)]^{|B_{(2,2)(3,3)}(\Psi)|} \\
&\times [(2)(4) + (4)(3)]^{|B_{(2,3)(3,4)}(\Psi)|} \times [(2)(5) + (3)(3)]^{|B_{(2,3)(3,5)}(\Psi)|} \times [(2)(4) + (3)(4)]^{|B_{(2,3)(4,4)}(\Psi)|} \\
&\times [(2)(5) + (3)(4)]^{|B_{(2,3)(4,5)}(\Psi)|} \times [(3)(5) + (3)(4)]^{|B_{(3,3)(4,5)}(\Psi)|} \times [(3)(8) + (4)(5)]^{|B_{(3,4)(5,8)}(\Psi)|}| \\
&= [(2)(3) + (2)(2)]^{4a+12} \times [(2)(3) + (2)(3)]^{12a+4} \times [(2)(4) + (4)(3)]^{24a+8} \\
&\times [(2)(5) + (3)(3)]^{4a+12} \times [(2)(4) + (3)(4)]^{9a+3} \times [(2)(5) + (3)(4)]^{12a+4} \\
&\times [(3)(5) + (3)(4)]^{12a+4} \times [(3)(8) + (4)(5)]^{8a+8} = [6 + 4]^{4a+12} \times [6 + 6]^{12a+4} \times [8 + 12]^{24a+8} \\
&\times [10 + 9]^{4a+12} \times [8 + 12]^{9a+3} \times [10 + 12]^{12a+4} \times [15 + 12]^{12a+4} \times [24 + 20]^{8a+8} \\
&= [10]^{4a+12} \times [12]^{12a+4} \times [20]^{24a+8} \times [19]^{4a+12} \times [20]^{9a+3} \times [22]^{12a+4} \times [27]^{12a+4} \times [44]^{8a+8} \\
&= [190]^{4a+12} \times [7128]^{12a+4} \times [20]^{33a+11} \times [44]^{8a+8}
\end{aligned}$$

Theorem 3.2. *Let $\Psi = ZnOx$ be a molecular structure of zinc oxide graph of growth $a \ge 1$. Then, the expression to compute the modified 2nd MZCI is given as*:

$$Z^M C_2^\star(\Psi) = [210]^{(4a+12)} \times [7452]^{(12a+4)} \times [22]^{(24a+8)} \times [20]^{(9a+3)} \times [55]^{(8a+8)}$$

Table 1: Total number of edges on degree and connection bases

$\lvert B^d(\mu, \nu)(\Psi)\rvert$ (on degree bases)	$\lvert B(\lambda, \vartheta)(\Psi)\rvert$ (on connection bases)	$\lvert B(\mu,\nu)(\lambda,\vartheta)(\Psi)\rvert$
$\lvert B^d_{(2,2)}(\Psi)\rvert = 4a + 12$	$\lvert B_{(2,3)}(\Psi)\rvert = 4a + 12$	$\lvert B_{(2,2)(2,3)}(\Psi)\rvert = 4a + 12$
$\lvert B^d_{(2,2)}(\Psi)\rvert = 12a + 4$	$\lvert B_{(3,3)}(\Psi)\rvert = 12a + 4$	$\lvert B_{(2,2)(3,3)}(\Psi)\rvert = 12a + 4$
$\lvert B^d_{(2,3)}(\Psi)\rvert = 24a + 8$	$\lvert B_{(3,4)}(\Psi)\rvert = 24a + 8$	$\lvert B_{(2,3)(3,4)}(\Psi)\rvert = 24a + 8$
$\lvert B^d_{(2,3)}(\Psi)\rvert = 4a + 12$	$\lvert B_{(3,5)}(\Psi)\rvert = 4a + 12$	$\lvert B_{(2,3)(3,5)}(\Psi)\rvert = 4a + 12$
$\lvert B^d_{(2,3)}(\Psi)\rvert = 9a + 3$	$\lvert B_{(4,4)}(\Psi)\rvert = 9a + 3$	$\lvert B_{(2,3)(4,4)}(\Psi)\rvert = 9a + 3$
$\lvert B^d_{(2,3)}(\Psi)\rvert = 12a + 4$	$\lvert B_{(4,5)}(\Psi)\rvert = 12a + 4$	$\lvert B_{(2,3)(4,5)}(\Psi)\rvert = 12a + 4$
$\lvert B^d_{(3,3)}(\Psi)\rvert = 12a + 4$	$\lvert B_{(4,5)}(\Psi)\rvert = 12a + 4$	$\lvert B_{(3,3)(4,5)}(\Psi)\rvert = 12a + 4$
$\lvert B^d_{(3,4)}(\Psi)\rvert = 8a + 8$	$\lvert B_{(5,8)}(\Psi)\rvert = 8a + 8$	$\lvert B_{(3,4)(5,8)}(\Psi)\rvert = 8a + 8$

Proof. After placing the computed values of $|B_{(\mu,\nu)(\lambda,\vartheta)}(\Psi)|$ from Table 1 in Eq. 2, we have:

$$
\begin{aligned}
Z^M C_2^\star(\Psi) &= \prod_{\substack{\lambda\le\beta\in N\\ \mu\le\nu\in N}} [\mu\lambda + \nu\beta]^{|B_{(\mu,\nu)(\lambda,\beta)}(\Psi)|} = [(2)(2) + (2)(3)]^{|B_{(2,2)(2,3)}(\Psi)|} \times [(2)(3) + (2)(3)]^{|B_{(2,2)(3,3)}(\Psi)|} \\
&\quad \times [(2)(3) + (4)(4)]^{|B_{(2,3)(3,4)}(\Psi)|} \times [(2)(3) + (3)(5)]^{|B_{(2,3)(3,5)}(\Psi)|} \times [(2)(4) + (3)(4)]^{|B_{(2,3)(4,4)}(\Psi)|} \\
&\quad \times [(2)(4) + (3)(5)]^{|B_{(2,3)(4,5)}(\Psi)|} \times [(3)(5) + (3)(4)]^{|B_{(3,3)(4,5)}(\Psi)|} \times [(3)(5) + (4)(8)]^{|B_{(3,4)(5,8)}(\Psi)|} \\
&= [(2)(2) + (2)(3)]^{4a+12} \times [(2)(3) + (2)(3)]^{12a+4} \times [(2)(3) + (4)(4)]^{24a+8} \\
&\quad \times [(2)(3) + (3)(5)]^{4a+12} \times [(2)(4) + (3)(4)]^{9a+3} \times [(2)(4) + (3)(5)]^{12a+4} \\
&\quad \times [(3)(4) + (3)(5)]^{12a+4} \times [(3)(5) + (4)(8)]^{8a+8} \\
&= [4 + 6]^{4a+12} \times [6 + 6]^{12a+4} \times [6 + 16]^{24a+8} \times [6 + 15]^{4a+12} \times [8 + 12]^{9a+3} \times [8 + 15]^{12a+4} \\
&\quad \times [12 + 15]^{12a+4} \times [15 + 40]^{8a+8} \\
&= [10]^{4a+12} \times [12]^{12a+4} \times [22]^{24a+8} \times [21]^{4a+12} \times [20]^{9a+3} \times [23]^{12a+4} \times [27]^{12a+4} \times [55]^{8a+8} \\
&= [210]^{4a+12} \times [7452]^{12a+4} \times [22]^{24a+8} \times [20]^{9a+3} \times [55]^{8a+8}
\end{aligned}
$$

Theorem 3.3. *Let $\Psi = ZnOx$ be a molecular structure of zinc oxide graph of growth $a \ge 1$. Then, the expression to compute the modified 3rd MZCI is given as*:

$$
\begin{aligned}
Z^M C_3^\star(\Psi) &= [24]^{4a+12} \times [36]^{12a+4} \times [96]^{24a+8} \times [90]^{4a+12} \\
&\quad \times [96]^{9a+3} \times [120]^{12a+4} \times [180]^{12a+4} \times [600]^{8a+8}
\end{aligned}
$$

Proof. After placing the values of $|B_{(\mu,\nu)(\lambda,\vartheta)}(\Psi)|$ from Table 1 in Eq. 3, we have:

$$
\begin{aligned}
Z^M C_3^\star(\Psi) &= \prod_{\substack{0\le\lambda\le\beta\le a-2\\ 0\le\mu\le\nu\le a-2}} [\mu\lambda \times \nu\beta]^{|B_{(\mu,\nu)(\lambda,\beta)}(\Psi)|} = [(2)(2) \times (2)(3)]^{|B_{(2,2)(2,3)}(\Psi)|} \times [(2)(3) \times (2)(3)]^{|B_{(2,2)(3,3)}(\Psi)|} \\
&\quad \times [(2)(3) \times (4)(4)]^{|B_{(2,3)(3,4)}(\Psi)|} \times [(2)(3) \times (3)(5)]^{|B_{(2,3)(3,5)}(\Psi)|} \times [(2)(4) \times (3)(4)]^{|B_{(2,3)(4,4)}(\Psi)|} \\
&\quad \times [(2)(4) \times (3)(5)]^{|B_{(2,3)(4,5)}(\Psi)|} \times [(3)(5) \times (3)(4)]^{|B_{(3,3)(4,5)}(\Psi)|} \times [(3)(5) \times (4)(8)]^{|B_{(3,4)(5,8)}(\Psi)|}| \\
&= [(2)(2) \times (2)(3)]^{4a+12} \times [(2)(3) \times (2)(3)]^{12a+4} \times [(2)(3) \times (4)(4)]^{24a+8} \\
&\quad \times [(2)(3) \times (3)(5)]^{4a+12} \times [(2)(4) \times (3)(4)]^{9a+3} \times [(2)(4) \times (3)(5)]^{12a+4} \\
&\quad \times [(3)(4) \times (3)(5)]^{12a+4} \times [(3)(5) \times (4)(8)]^{8a+8} = [4 \times 6]^{4a+12} \times [6 \times 6]^{12a+4} \times [6 \times 16]^{24a+8} \times [6 \times 15]^{4a+12} \\
&\quad \times [8 \times 12]^{9a+3} \times [8 \times 15]^{12a+4} \times [12 \times 15]^{12a+4} \times [15 \times 40]^{8a+8} \\
&= 24^{4a+12} \times [36]^{12a+4} \times [96]^{24a+8} \times [90]^{4a+12} \times [96]^{9a+3} \times [120]^{12a+4} \times [180]^{12a+4} \times [600]^{8a+8}
\end{aligned}
$$

4 Connection-based ZIs of zinc silicate

This section includes all the main results for modified 1st MZCI, modified 2nd MZCI, and modified 3rd MZCI of molecular graph of ZnSl of growth a. Let, $\Gamma = \mathrm{ZnSl}(a)$ be a molecular graph of zinc oxide of growth a. The cardinality of the vertices and edges of the molecular graph Γ is $82a + 50$ and $103a + 61$, respectively. The connection-based molecular graph of ZnSl for $a = 1, 2, 3$ is depicted in Figures 4–6.

For our ease, we divide the structure of ZnSl into diamond structure of hexagons and ξ hexagons:

1. Diamond structure of hexagons: A structure in which four hexagons are joined in such a way that they have one common vertex having CN 8 and two outer vertices having CN 2 is considered to be diamond structure of hexagons.

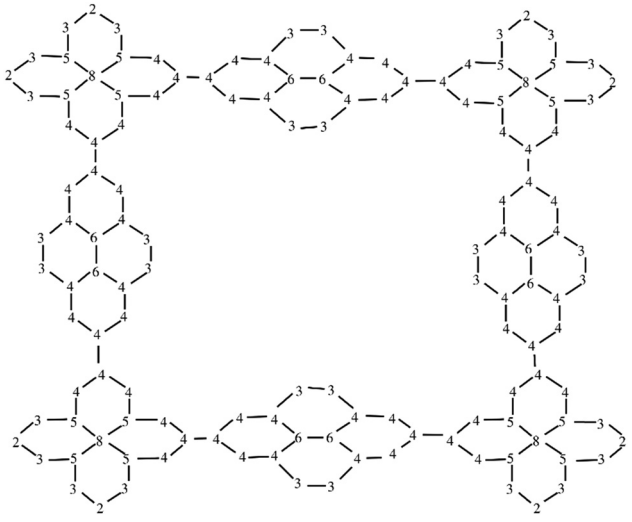

Figure 4: Molecular structure of ZnSl graph for $a = 1$.

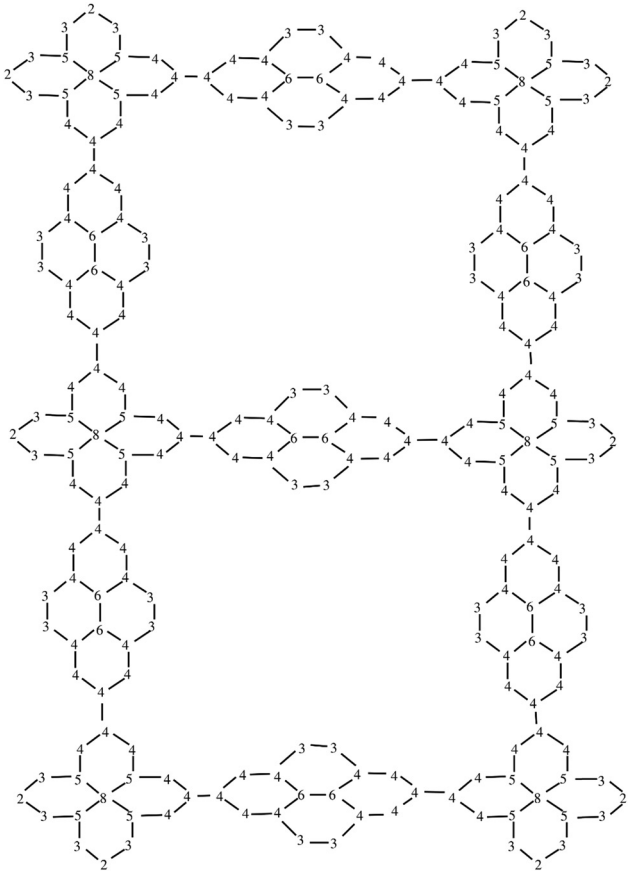

Figure 5: Molecular structure of ZnSl graph for $a = 2$.

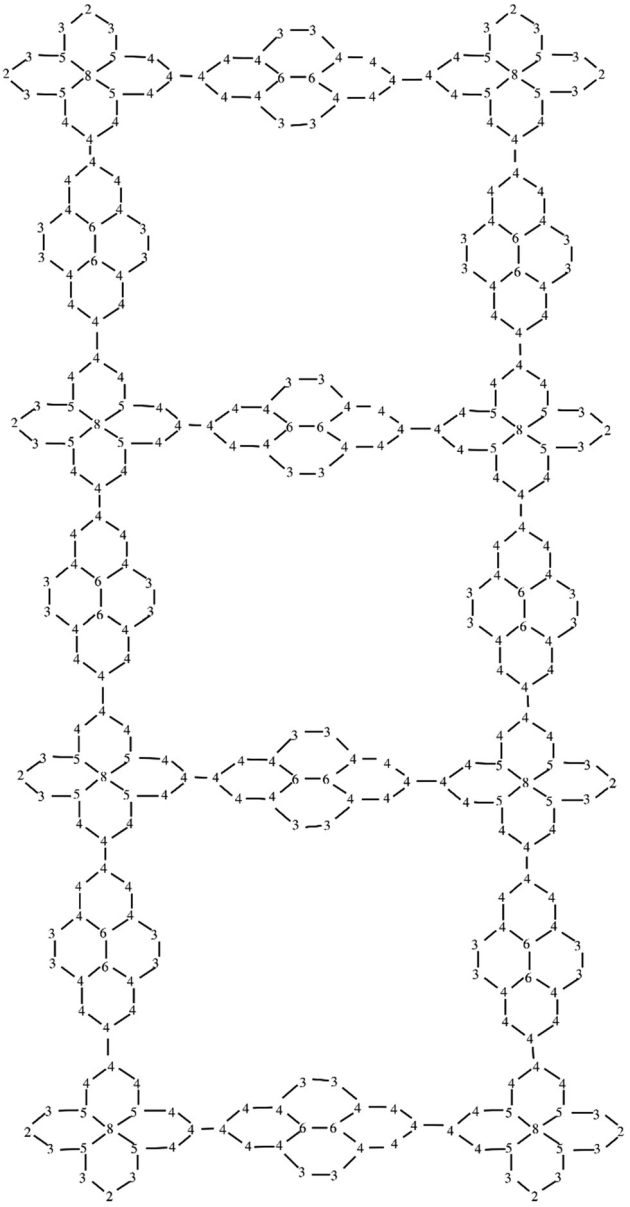

Figure 6: Molecular structure of ZnSl graph for $a = 3$.

2. Star structure of hexagons: A structure in which four hexagons are joined in such a way that they have one common vertex having CN 8 and one outer vertex having CN 2 is considered to be star structure of hexagons.
3. *D* structure of hexagon: The structure of hexagons which is not diamond structure or star structure is considered to be *D* structure of hexagons.

The number of diamond structure of hexagons, star structure of hexagons, and ξ hexagons are given in following:

- Number of diamond structure of hexagons = 4,
- Number of star structure of hexagons = $2a - 2$,
- Number of *D* structure of hexagons = $3a + 1$.

Theorem 4.1. *Let* $\Gamma = ZnSl$ *be a molecular structure of zinc oxide graph of growth* $a \geq 1$. *Then, the expression to compute the modified 1st MZCI is given as*:

$$Z^M C_1^\star(\Gamma) = [190]^{4a+12} \times [11220]^{12a+4} \times [12]^{6a+2} \times [24]^{6a+12} \times [20]^{36a+12} \times [36]^{3a+1} \times [44]^{8a+8}$$

Proof. Firstly, we make the partitions of edges with respect to the degree of incident vertices. There are following four partitions of edges with respect to the degrees of incident vertices:

$$P_1^d = B_{2,2}^d(\Gamma) = \{e = mz \in T : d_\Gamma(m) = 2,\ d_\Gamma(z) = 2\}$$
$$P_2^d = B_{2,3}^d(\Gamma) = \{e = mz \in T : d_\Gamma(m) = 2,\ d_\Gamma(z) = 3\}$$
$$P_3^d = B_{3,3}^d(\Gamma) = \{e = mz \in T : d_\Gamma(m) = 3,\ d_\Gamma(z) = 3\}$$
$$P_4^d = B_{3,4}^d(\Gamma) = \{e = mz \in T : d_\Gamma(m) = 3,\ d_\Gamma(z) = 4\}$$

The cardinalities of these partitioned edges are given below:

$$|B_{3,4}(\Psi)| = 24a + 8$$
$$|B_{3,5}(\Psi)| = 4a + 12$$
$$|B_{4,4}(\Psi)| = 4a + 12$$
$$|B_{4,5}(\Psi)| = 12a + 4$$
$$|B_{5,8}(\Psi)| = 8a + 8$$

Further, we divide the edges of Γ based on their CNs. We have the following seven partitions for the edges as given below:

$$P_1^e = B_{2,3}(\Gamma) = \{e = mz \in T : \vartheta_\Gamma(m) = 2,\ \vartheta_\Gamma(z) = 3\}$$
$$P_2^e = B_{3,3}(\Gamma) = \{e = mz \in T : \vartheta_\Gamma(m) = 3,\ \vartheta_\Gamma(z) = 3\}$$
$$P_3^e = B_{3,4}(\Gamma) = \{e = mz \in T : \vartheta_\Gamma(m) = 3,\ \vartheta_\Gamma(z) = 4\}$$
$$P_4^e = B_{3,5}(\Gamma) = \{e = mz \in T : \vartheta_\Gamma(m) = 3,\ \vartheta_\Gamma(z) = 5\}$$
$$P_5^e = B_{4,4}(\Gamma) = \{e = mz \in T : \vartheta_\Gamma(m) = 4,\ \vartheta_\Gamma(z) = 4\}$$
$$P_6^e = B_{4,5}(\Gamma) = \{e = mz \in T : \vartheta_\Gamma(m) = 4,\ \vartheta_\Gamma(z) = 5\}$$
$$P_7^e = B_{4,6}(\Gamma) = \{e = mz \in T : \vartheta_\Gamma(m) = 4,\ \vartheta_\Gamma(z) = 6\}$$
$$P_8^e = B_{5,8}(\Gamma) = \{e = mz \in T : \vartheta_\Gamma(m) = 5,\ \vartheta_\Gamma(z) = 8\}$$
$$P_7^e = B_{6,6}(\Gamma) = \{e = mz \in T : \vartheta_\Gamma(m) = 6,\ \vartheta_\Gamma(z) = 6\}$$

Now, we compute $|B_{2,3}(\Gamma)|$. One can easily see that (2,3)-type edges exist in diamond and star structures of hexagons. The number of (2,3)-type edges in diamond structure is four, while in star structure, it is 2.

Thus, we have

$$|B_{(2,3)}(\text{diamond structure of hexagons})| = 4 \times 4 = 16$$
$$|B_{(2,3)}(\text{star structure of hexagons})| = 2(2a - 2)$$
$$|B_{(2,3)}(\Gamma)| = 16 + 4a - 4, = 4a + 12$$

Next, we compute $|B_{3,3}(\Gamma)|$. As it can be seen that only the *D* structure of hexagons contains the (3,3)-type edges in Γ. Thus, we have:

$$|B_{(3,3)}(D \text{ structure of hexagons})| = 2(3a + 1)$$
$$|B_{(3,3)}(\Gamma)| = 6a + 2$$

Similarly, we can calculate the other edges. The cardinalities of the other type of edges are:

$$|B_{3,4}(\Gamma)| = 12a + 4, \quad |B_{3,5}(\Gamma)| = 4a + 12$$
$$|B_{4,4}(\Gamma)| = 42a + 14, \quad |B_{4,5}(\Gamma)| = 12a + 4$$
$$|B_{4,6}(\Gamma)| = 12a + 14 \quad |B_{5,8}(\Gamma| = 8a + 8$$
$$|B_{6,6}(\Gamma)| = 3a + 1$$

Now, in order to compute modified 1st MZCI, modified 2nd MZCI, and modified 3rd MZCI, we split the partitioned degree-based edges with respect to the connection-based edges.

Table 2 shows the cardinality of edges with degree (μ, ν) and CNs (λ, ϑ). By placing the values of $|B_{(\mu,\nu)(\lambda,\vartheta)}(\Gamma)|$ in Eq. 1, we have:

$$
\begin{aligned}
Z\,{}^{M}C_1^{\star}(Q) &= \prod_{\substack{\lambda\le\beta\in N\\ \mu\le\nu\in N}} [\mu\beta+\nu\lambda]^{|B_{(\mu,\nu)(\lambda,\beta)}(Q)|} = [(2)(3)+(2)(2)]^{|B_{(2,2)(2,3)}(\Gamma)|}\times[(2)(3)+(2)(3)]^{|B_{(2,2)(3,3)}(\Gamma)|}\\
&\times[(2)(4)+(3)(3)]^{|B_{(2,3)(3,4)}(\Gamma)|}\times[(2)(5)+(3)(3)]^{|B_{(2,3)(3,5)}(\Gamma)|}\times[(2)(4)+(3)(4)]^{|B_{(2,3)(4,4)}(\Gamma)|}\\
&\times[(2)(5)+(3)(4)]^{|B_{(2,3)(4,5)}(\Gamma)|}\times[(3)(4)+(3)(4)]^{|B_{(3,3)(4,4)}(\Gamma)|}\times[(3)(6)+(3)(4)]^{|B_{(3,3)(4,6)}(\Gamma)|}\\
&\times[(3)(6)+(3)(6)]^{|B_{(3,3)(6,6)}(\Gamma)|}\times[(3)(8)+(4)(5)]^{|B_{(3,4)(5,8)}(\Gamma)|}\\
&= [(2)(3)+(2)(2)]^{4a+12}\times[(2)(3)+(2)(3)]^{6a+2}\times[(2)(4)+(3)(3)]^{12a+4}\times[(2)(5)+(3)(3)]^{4a+12}\\
&\times[(2)(4)+(3)(4)]^{36a+12}\times[(2)(5)+(3)(4)]^{12a+4}\times[(3)(4)+(3)(4)]^{6a+12}\times[(3)(6)+(3)(4)]^{12a+4}\\
&\times[(3)(6)+(3)(6)]^{3a+1}\times[(3)(8)+(4)(5)]^{8a+8} = [6+4]^{4a+12}\times[6+6]^{6a+2}\times[8+9]^{12a+4}\times[10+9]^{4a+12}\\
&\times[8+12]^{36a+12}\times[10+12]^{12a+4}\times[12+12]^{6a+12}\times[18+12]^{12a+4}\times[18+18]^{3a+1}\times[24+20]^{8a+8}\\
&= [10]^{4a+12}\times[12]^{6a+2}\times[17]^{12a+4}\times[19]^{4a+12}\times[20]^{36a+12}\times[22]^{12a+4}\times[24]^{6a+12}\\
&\times[30]^{12a+4}\times[36]^{3a+1}\times[44]^{8a+8} = [190]^{4a+12}\times[11220]^{12a+4}\times[12]^{6a+2}\times[24]^{6a+12}\times[20]^{36a+12}\times[36]^{3a+1}\\
&\times[44]^{8a+8}
\end{aligned}
$$

Theorem 4.2. *Let* $\Gamma = ZnSl$ *be a molecular structure of zinc oxide graph of growth* $a \ge 1$. *Then, the expression to compute the modified 2nd MZCI is given as*:

$$
\begin{aligned}
Z^{M}C_2^{\star}(\Gamma) &= [210]^{4a+12}\times[11880]^{12a+4}\times[12]^{6a+2}\\
&\times[24]^{6a+12}\times[20]^{36a+12}\times[36]^{3a+1}\times[47]^{8a+8}
\end{aligned}
$$

Proof. After placing the values of $|B_{(\mu,\nu)(\lambda,\vartheta)}(\Gamma)|$ from Table 2 in Eq. 2, we have:

$$
\begin{aligned}
Z^{M}C_2^{\star}(Q) &= \prod_{\substack{\lambda\le\beta\in N\\ \mu\le\nu\in N}} [\mu\lambda+\nu\beta]^{|B_{(\mu,\nu)(\lambda,\beta)}(Q)|} = [(2)(2)+(2)(3)]^{|B_{(2,2)(2,3)}(\Gamma)|}\\
&\times[(2)(3)+(2)(3)]^{|B_{(2,2)(3,3)}(\Gamma)|}\times[(2)(3)+(3)(4)]^{|B_{(2,3)(3,4)}(\Gamma)|}\\
&\times[(2)(3)+(3)(5)]^{|B_{(2,3)(3,5)}(\Gamma)|}\times[(2)(4)+(3)(4)]^{|B_{(2,3)(4,4)}(\Gamma)|}\\
&\times[(2)(4)+(3)(5)]^{|B_{(2,3)(4,5)}(\Gamma)|}\times[(3)(4)+(3)(4)]^{|B_{(3,3)(4,4)}(\Gamma)|}\\
&\times[(3)(4)+(3)(6)]^{|B_{(3,3)(4,6)}(\Gamma)|}\times[(3)(6)+(3)(6)]^{|B_{(3,3)(6,6)}(\Gamma)|}\\
&\times[(3)(5)+(4)(8)]^{|B_{(3,4)(5,8)}(\Gamma)|} = [(2)(2)+(2)(3)]^{4a+12}\times[(2)(3)+(2)(3)]^{6a+2}\\
&\times[(2)(3)+(3)(4)]^{12a+4}\times[(2)(3)+(3)(5)]^{4a+12}\times[(2)(4)+(3)(4)]^{36a+12}\\
&\times[(2)(4)+(3)(5)]^{12a+4}\times[(3)(4)+(3)(4)]^{6a+12}\times[(3)(4)+(3)(6)]^{12a+4}\\
&\times[(3)(6)+(3)(6)]^{3a+1}\times[(3)(5)+(4)(8)]^{8a+8} = [4+6]^{4a+12}\times[6+6]^{6a+2}\\
&\times[6+12]^{12a+4}\times[6+15]^{4a+12}\times[8+12]^{36a+12}\\
&\times[8+15]^{12a+4}\times[12+12]^{6a+12}\times[12+18]^{12a+4}\times[18+18]^{3a+1}\\
&\times[15+32]^{8a+8}\\
&= [10]^{4a+12}\times[12]^{6a+2}\times[18]^{12a+4}\times[21]^{4a+12}\times[20]^{36a+12}\times[22]^{12a+4}\times[24]^{6a+12}\times[30]^{12a+4}\times[36]^{3a+1}\\
&\times[47]^{8a+8} = [210]^{4a+12}\times[11880]^{12a+4}\times[12]^{6a+2}\times[24](6a+12)\times[20]^{36a+12}\times[36]^{3a+1}\times[47]^{8a+8}
\end{aligned}
$$

Theorem 4.3. *Let* $\Gamma = ZnSl$ *be a molecular structure of zinc oxide graph of growth* $a \ge 1$. *Then, the expression to compute the modified 3rd MZCI is given as*:

$$
\begin{aligned}
Z^{M}C_3^{\star}(\Gamma) &= [2160]^{4a+12}\times[1866240]^{12a+4}\times[36]^{6a+2}\\
&\times[144]^{6a+12}\times[96]^{36a+12}\times[324]^{3a+1}\\
&\times[480]^{8a+8}
\end{aligned}
$$

Proof. After placing the values of $|B_{(\mu,\nu)(\lambda,\vartheta)}(\Gamma)|$ from Table 2 in Eq. 3, we have:

$$
\begin{aligned}
Z^M C_3^*(\Gamma) &= \prod_{\substack{\lambda\le\beta\in N\\ \mu\le\nu\in N}} [\mu\lambda\times\nu\beta]^{|B_{(\mu,\nu)(\lambda,\beta)}(\Gamma)|} = [(2)(2)\times(2)(3)]^{|B_{(2,2)(2,3)}(\Gamma)|}\times[(2)(3)\times(2)(3)]^{|B_{(2,2)(3,3)}(\Gamma)|}\\
&\times[(2)(3)\times(3)(4)]^{|B_{(2,3)(3,4)}(\Gamma)|}\times[(2)(3)\times(3)(5)]^{|B_{(2,3)(3,5)}(\Gamma)|}\times[(2)(4)\times(3)(4)]^{|B_{(2,3)(4,4)}(\Gamma)|}\\
&\times[(2)(4)\times(3)(5)]^{|B_{(2,3)(4,5)}(\Gamma)|}\times[(3)(4)\times(3)(4)]^{|B_{(3,3)(4,4)}(\Gamma)|}\times[(3)(4)\times(3)(6)]^{|B_{(3,3)(4,6)}(\Gamma)|}\\
&\times[(3)(6)\times(3)(6)]^{|B_{(3,3)(6,6)}(\Gamma)|}\times[(3)(5)\times(4)(8)]^{|B_{(3,4)(5,8)}(\Gamma)|} = [(2)(2)\times(2)(3)]^{4a+12}\times[(2)(3)\times(2)(3)]^{6a+2}\\
&\times[(2)(3)\times(3)(4)]^{12a+4}\times[(2)(3)\times(3)(5)]^{4a+12}\times[(2)(4)\times(3)(4)]^{36a+12}\times[(2)(4)\times(3)(5)]^{12a+4}\\
&\times[(3)(4)\times(3)(4)]^{6a+12}\times[(3)(4)\times(3)(6)]^{12a+4}\times[(3)(6)\times(3)(6)]^{3a+1}\times[(3)(5)\times(4)(8)]^{8a+8}\\
&= [4\times6]^{4a+12}\times[6\times6]^{6a+2}\times[6\times12]^{12a+4}\times[6\times15]^{4a+12}\times[8\times12]^{36a+12}\times[8\times15]^{12a+4}\times[12\times12]^{6a+12}\\
&\times[12\times18]^{12a+4}\times[18\times18]^{3a+1}\times[15\times32]^{8a+8} = [24]^{4a+12}\times[36]^{6a+2}\times[72]^{12a+4}\times[90]\hat{}(4a\\
&+12)\times[96]\hat{}(36a+12)\times[120]^{12a+4}\times[144]^{6a+12}\times[216]^{12a+4}\times[324]^{3a+1}\times[480]^{8a+8} = [2160]^{4a+12}\\
&\times[1866240]^{12a+4}\times[36]^{6a+2}\times[144]^{6a+12}\times[96]^{36a+12}\times[324]^{3a+1}\times[480]^{8a+8}
\end{aligned}
$$

Table 2: Total number of edges on degree and connection bases

$\lvert B^d(\mu,\nu)(\Gamma)\rvert$	$\lvert B(\lambda,\vartheta)(\Gamma)\rvert$	$\lvert B(\mu,\nu)(\lambda,\vartheta)(\Gamma)\rvert$
(on degree bases)	(on connection bases)	
$\lvert B^d_{2,2}(\Gamma)\rvert = 4a + 12$	$\lvert B_{2,3}(\Gamma)\rvert = 4a + 12$	$\lvert B_{(2,2)(2,3)}(\Gamma)\rvert = 4a + 12$
$\lvert B^d_{2,2}(\Gamma)\rvert = 6a + 2$	$\lvert B_{3,3}(\Gamma)\rvert = 6a + 2$	$\lvert B_{(2,2)(3,3)}(\Gamma)\rvert = 6a + 2$
$\lvert B^d_{2,3}(\Gamma)\rvert = 12a + 4$	$\lvert B_{3,4}(\Gamma)\rvert = 12a + 4$	$\lvert B_{(2,3)(3,4)}(\Gamma)\rvert = 12a + 4$
$\lvert B^d_{2,3}(\Gamma)\rvert = 4a + 12$	$\lvert B_{3,4}(\Gamma)\rvert = 4a + 12$	$\lvert B_{(2,3)(3,5)}(\Gamma)\rvert = 4a + 12$
$\lvert B^d_{2,3}(\Gamma)\rvert = 36a + 12$	$\lvert B_{4,4}(\Gamma)\rvert = 36a + 12$	$\lvert B_{(2,3)(4,4)}(\Gamma)\rvert = 36a + 12$
$\lvert B^d_{2,3}(\Gamma)\rvert = 12a + 4$	$\lvert B_{4,5}(\Gamma)\rvert = 12a + 4$	$\lvert B_{(2,3)(4,5)}(\Gamma)\rvert = 12a + 4$
$\lvert B^d_{3,3}(\Gamma)\rvert = 6a + 12$	$\lvert B_{4,4}(\Gamma)\rvert = 6a + 12$	$\lvert B_{(3,3)(4,4)}(\Gamma)\rvert = 6a + 12$
$\lvert B^d_{3,3}(\Gamma)\rvert = 12a + 4$	$\lvert B_{4,6}(\Gamma)\rvert = 12a + 4$	$\lvert B_{(3,3)(4,6)}(\Gamma)\rvert = 12a + 4$
$\lvert B^d_{3,3}(\Gamma)\rvert = 3a + 1$	$\lvert B_{6,6}(\Gamma)\rvert = 3a + 1$	$\lvert B_{(3,3)(6,6)}(\Gamma)\rvert = 3a + 1$
$\lvert B^d_{3,4}(\Gamma)\rvert = 8a + 8$	$\lvert B_{5,8}(\Gamma)\rvert = 8a + 8$	$\lvert B_{(3,4)(5,8)}(\Gamma)\rvert = 8a + 8$

Table 3: Comparison between the values of ZnOx- and ZnSl-related MOFs

	$Z^M C_1^*(\Psi)$	$[190]^{4a+12}\times[7128]^{12a+4}\times[20]^{33a+11}\times[44]^{8a+8}$
ZnOx-related	$Z^M C_2^*(\Psi)$	$[210]^{4a+12}\times[7452]^{12a+4}\times[22]^{24a+8}\times[20]^{9a+3}\times[55]^{8a+8}$
MOFs	$Z^M C_3^*(\Psi)$	$[24]^{4a+12}\times[36]^{12a+4}\times[96]^{24a+8}\times[90]^{4a+12}\times[96]^{9a+3}$ $\times[120]^{12a+4}\times[180]^{12a+4}\times[600]^{8a+8}$
	$Z^M C_1^*(\Gamma)$	$[190]^{4a+12}\times[11220]^{12a+4}\times[12]^{6a+2}\times[24]^{6a+12}\times[20]^{36a+12}$ $\times[36]^{3a+1}\times[44]^{8a+8}$
ZnSl-related	$Z^M C_3^*(\Gamma)$	$[210]^{4a+12}\times[11880]^{12a+4}\times[12]^{6a+2}\times[24](6a+12)\times[20]^{36a+12}$ $\times[36]^{3a+1}\times[47]^{8a+8}$
MOFs	$Z^M C_3^*(\Gamma)$	$[2160]^{4a+12}\times[1866240]^{12a+4}\times[36]^{6a+2}\times[144]^{6a+12}\times[96]^{36a+12}$ $\times[324]^{3a+1}\times[480]^{8a+8}$

5 Comparative analysis and concluding remarks

In this section, we compare ZnOx- and ZnSl-related MOFs via some MZCIs, namely modified 1st MZCI, modified 2nd MZCI, and modified 3rd MZCI. The computed values of MZCIs for ZnOx- and ZnSl-related MOFs are given in Table 3.

From Table 3, it can be concluded that modified 3rd MZCI attains the maximum value than all the other MZCIs for both ZnOx- and ZnSl-related MOFs. Thus, modified 3rd MZCI has larger ability to predict the physical and chemical properties of MOFs. On the other side, all computed values for zinc silicate-related MOFs are higher than zinc oxide-related MOFs. Thus, zinc silicate-related MOFs are better than zinc oxide-related MOFs.

The concluding remarks are as follows:

1. MOFs are recently developed porous chemical compounds having vast range of utilizations in absorption analysis, heterogeneous catalysis, sensing, environmental hazard, super-capacitors, gas storage device, and the assessment of different chemicals. Zinc-related MOFs are widely utilized in medical applications such as biosensing, drug delivery, and cancer imaging.
2. TIs, the numerical graph descriptors are useful in characterizing the topology of molecular structures and helpful in defining the psychochemical properties of these structures. The ZCI, rather than the other classical degree and distance-based ZIs, have better applicability to specify the physical and chemical properties of molecular structures.
3. In this article, we have compared two zinc-related MOFs, namely, ZnOx and ZnSl via some multiplicative Zagreb indices (MZIs), namely modified first MZCI (1st MZCI), modified second MZCI (2nd MZCI), and modified third MZCI (3rd MZCI). We have observed from the comparison that the modified 3rd MZCI attains the maximum value than the other MZCIs.

Acknowledgment: The authors are very grateful to the anonymous referees for their valuable comments and suggestion that improved the quality of this paper.

Funding information: The authors state no funding involved.

Author contributions: Muhammad Javaid: writing – final draft, writing – review and editing, formal analysis, visualization; Aqsa Sattar: writing – initial draft, data collection, methodology.

Conflict of interest: Muhammad Javaid is a Guest Editor of the Main Group Metal Chemistry's Special Issue "Theoretical and computational aspects of graph-theoretic methods in modern-day chemistry" in which this article is published.

Data availability statement: The data used to support the finding of this study are cited at relevant places within the text as references.

References

Abbas G., Ibrahim M., Ahmad A., Azeem M., Elahi K., M-polynomials of tetra-cyano-benzene transition metal structure. Polycycl. Aromatic Compd., 2021, 1–11. doi: 10.1080/10406638.2021.2019797.

Ahmad A., Asim M.A., Nadeem M.F. Polynomials of degree-based indices of metal-organic networks. Combinatorial Chem. High. Throughput Screen., 2022, 25(3), 510–518.

Ali A., Gutman I., Milovanovic E., Milovanovic I. Sum of powers of the degrees of graphs: extremal results and bounds. MATCH Commun. Math. Comput. Chem., 2018, 80(1), 5–84.

Ali U., Javaid M., Kashif A. Modified Zagreb connection indices of the T-sum graphs. Main. Group. Met. Chem., 2020, 43(1), 43–55.

Ali A., Trinajstić N. A novel/old modification of the first Zagreb index. Mol. Inf., 2018, 37(6–7), 1800008.

Awais H.M., Jamal M., Javaid M. Topological properties of metal-organic frameworks. Main. Group. Met. Chem., 2020, 43(1), 67–76.

Chu Y.M., Abid M., Qureshi M.I., Fahad A., Aslam A. Irregular topological indices of certain metal organic frameworks. Main. Group. Met. Chem., 2020, 44(1), 73–81.

Dhanalakshmi K., Amalorpava J., Benedict Michaelraj L. Modified and multiplicative zagreb indices on graph operators. J. Computer Math. Sci. 2016, 7(4), 225–232.

Ding G., Yuan J., Jin F., Zhang Y., Han L., Ling X., Ma W. High-performance all-polymer nonfullerene solar cells by employing an efficient polymer-small molecule acceptor alloy strategy. Nano Energy, 2017, 36, 356–365.

Dustigeer G., Ali H., Khan M.I., Chu Y.M. On multiplicative degree based topological indices for planar octahedron networks. Main. Group. Met. Chem., 2020, 43(1), 219–228,

Furtula B., Gutman I. A forgotten topological index. J. Math. Chem., 2015, 53(4), 1184–1190.

Gao W., Iqbal Z., Jaleel A., Aslam A., Ishaq M., Aamir M. Computing entire Zagreb indices of some dendrimer structures. Main. Group. Met. Chem., 2020, 43(1), 229–236,

Gutman I., Rusic B., Trinajstić N., Wilcox Jr C.F. Graph theory and molecular orbitals. XII. Acyclic polyenes. J. Chem. Phys., 1975, 62(9), 3399–3405.

Gutman I., Trinajstic N. Graph theory and molecular orbitals. Total φ-electron energy of alternant hydrocarbons. Chem. Phys. Lett., 1972, 17(4), 535–538.

Haoer R.S., Mohammed M.A., Selvarasan T., Chidambaram N., Devadoss N. Multiplicative leap Zagreb indices of T-thorny graphs. Eurasian Chem. Commun., 2020, 2(8), 841–846.

Hwang Y.K., Hong D.Y., Chang J.S., Jhung S.H., Seo Y.K., Kim J., Férey G. Amine grafting on coordinatively unsaturated metal centers of MOFs: consequences for catalysis and metal encapsulation. Angew. Chem., 2008, 120(22), 4212–4216.

Javaid M., Ali U., Siddiqui K. Novel, connection-based Zagreb indices of several wheel-related graphs. Comp. J. Comb. Math., 2021, 1, 1–28.

Javaid M., Imran M. Topological investigations of chemical networks. Main. Group. Met. Chem., 2021, 44(1), 267–269.

Kashif A., Aftab S., Javaid M., Awais H.M., M-polynomial-based topological indices of metal-organic networks. Main. Group. Met. Chem., 2021, 44(1), 129–140.

Kim M., Cahill J.F., Fei H., Prather K.A., Cohen S.M. Postsynthetic ligand and cation exchange in robust metal–organic frameworks. J. Am. Chem. Soc., 2012, 134(43), 18082–18088.

Li S., Shi L., Gao W. Two modified Zagreb indices for random structures. Main. Group. Met. Chem., 2021, 44(1), 150–156.

Lin R.B., Xiang S., Xing H., Zhou W., Chen B. Exploration of porous metal–organic frameworks for gas separation and purification. Coord. Chem. Rev., 2019, 378, 87–103.

Nikolic S., Kovacevic G., Milicevic A., Trinajstic N. The Zagreb indices 30 years after. Croatica Chem. Acta, 2003, 76(2), 113–124.

Prasad A.S. Zinc in human health: effect of zinc on immune cells. Mol. Med., 2008, 14(5), 353–357.

Rao Y., Kanwal A., Abbas R., Noureen S., Fahad A., Qureshi M.I. Some degree-based topological indices of caboxy-terminated dendritic macromolecule. Main. Group. Met. Chem., 2021, 44(1), 165–172.

Sattar A., Javaid M., Bonyah E. Connection-based multiplicative zagreb indices of dendrimer nanostars. J. Math., 2021, 2021.

Sattar A., Javaid M., Alam M.N. On the studies of dendrimers via connection based molecular descriptor, Math. Probl. Eng., 2022, 1–13.

Siddiqui M.K., Chu Y.-M., Nasir M., Nadeem M.F., Hanif M.F. On topological descriptors of ceria oxide and their applications. Main. Group. Met. Chem., 2021, 44(1), 103–116,

Taghipour T., Karimipour G., Ghaedi M., Asfaram A. Mild synthesis of a Zn (II) metal organic polymer and its hybrid with activated carbon: application as antibacterial agent and in water treatment by using sonochemistry: optimization, kinetic and isotherm study. Ultrason. Sonochem., 2018, 41, 389–396.

Thornton A.W., Nairn K.M., Hill J.M., Hill A.J., Hill M.R. Metal–organic frameworks impregnated with magnesium-decorated fullerenes for methane and hydrogen storage. J. Am. Chem. Soc., 2009, 131(30), 10662–10669.

Wang K., Yin Y., Li C., Geng Z., Wang Z. Facile synthesis of zinc (II)-carboxylate coordination polymer particles and their luminescent, biocompatible and antibacterial properties. Cryst. Eng. Comm., 2011, 13(20), 6231–6236.

Wiener H. Structural determination of paraffin boiling points. J. Am. Chem. Soc., 1947, 69(1), 17–20.

Xu G., Nie P., Dou H., Ding B., Li L., Zhang X. Exploring metal organic frameworks for energy storage in batteries and supercapacitors. Mater. Today, 2017, 20(4), 191–209.

Yap M.H., Fow K.L., Chen G.Z. Synthesis and applications of MOF-derived porous nanostructures. Green. Energy Env., 2017, 2(3), 218–245.

Yin Z., Zhou Y.L., Zeng M.H., Kurmoo M. The concept of mixed organic ligands in metal organic frameworks: design, tuning and functions. Dalton Trans., 44(12) (2015), 5258–5275.

Zahra N., Ibrahim M. On topological properties of hierarchical hypercube network based on Ve and Ev degree. Main. Group. Met. Chem., 2021, 44(1), 185–193.

Zhao D., Muhammad M.H., Siddiqui M.K., Nasir M., Nadeem M.F., Hanif M.F. Computation and analysis of topological co-indices for metal-organic compound. Curr. Org. Synth., 2021, 18(8), 750–760.